

ORIGINAL ARTICLE

Study of Optical and Structural Properties of SILAR-deposited Cobalt Sulphide Thin Films

C. B. Eze^a, I. A. Ezenwa^a, N. L. Okoli^{b,*}, C. I. Elekalachi^a, N. A. Okereke^a

^a Department of Industrial Physics, Chukwuemeka Odumegwu Ojukwu University, Uli Campus, Anambra State, Nigeria

^b Department of Physics, Legacy University Okija, Anambra State, Nigeria

KEYWORDS

Cobalt Sulphide,
SILAR Method,
Optical properties,
Structural properties,
Bandgap

ABSTRACT

Cobalt Sulphide (CoS) thin films were deposited on a non-conducting microscopic glass substrates using successive ionic layer adsorption and reaction (SILAR) technique at room temperature. The deposited CoS thin films were subjected to optical and structural characterizations. The absorbance result showed that cobalt sulphide films are moderately absorbing films with absorbance values ranging from 0.70 to 0.19. Transmittance results show that these deposited films are fairly transparent in visible light and near-infrared regions. Transmittance ranges from 19.8% to 63.9%. The transmittance decreased as the number of SILAR cycles increased. The reflectance of our synthesized films was generally low, with values ranging between 0.10 and 0.20. Our result also shows that within the UV and VIS region, refractive index decreased as the number of SILAR cycles increased for all the films deposited. Refractive index value ranges from 1.92 at 300 nm to its peak value of 2.64 at 1000 nm. The bandgap energy of the films deposited ranged from 2.00 – 2.30 eV. Optical thickness of the films ranges from 0.52 μm to 0.87 μm which shows an increase as the number of SILAR cycles increased. Structural analysis showed that the XRD pattern of deposited CoS thin films have peaks corresponding to the reflections of hexagonal phase of CoS with lattice parameter $a=b=3.377 \text{ \AA}$ and $c=5.150 \text{ \AA}$. The preferred orientation is along the [102] plane. Crystallite sizes, microstrain and dislocation density of the films obtained using Williamson–Hall plot method range from 32.25 to 40.78 nm, 2.0×10^{-4} to 7.0×10^{-4} and 9.61×10^{14} to 6.01×10^{14} lines/m² respectively.

ARTICLE HISTORY

Received: June 05, 2023

Revised: July 11, 2023

Accepted: August 19, 2023

Published: October 13, 2023

1 Introduction

Cobalt sulphide, known as chemical compounds with the formula Co_xS_y , possesses enhanced catalytic activity and is highly favored as a material for the counter electrode (CE) due to its electrocatalytic properties. Various well-studied types of cobalt sulphide minerals include CoS , CoS_2 , Co_3S_4 , and Co_9S_8 . Generally, cobalt sulphides are black, semiconducting substances that are insoluble in water and exhibit non-stoichiometric behavior. CoS , belonging to the II – IV group, is an intrinsic semiconductor and serves as a suitable candidate for thin films of metal sulphides. CoS , also referred to as cobalt sulphide, finds extensive applications in solar selective

coatings, infrared (IR) detectors, and as a storage electrode in photo-electrochemical storage devices. [1].

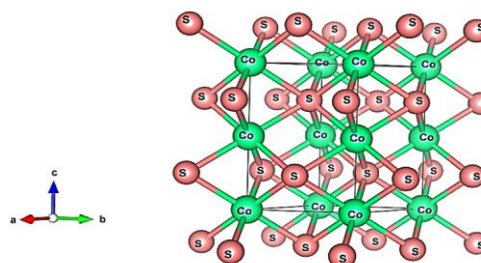


Figure 1: Structural arrangement of cobalt and sulphur atoms in cobalt sulphide system (VESTA)

* CORRESPONDING AUTHOR | N. L. Okoli, ✉ okolinonsolivinus@gmail.com

The complexity of the phase diagram in the CoS system arises from the simultaneous presence of highly reducible cobalt and easily oxidizable sulfur ions [2]. Figure 1 shows the structural arrangement of cobalt and sulphur atoms in cobalt sulphide system drawn using VESTA software. Cobalt sulphides are reported to have potential applications as catalysts [3]-[4] capable of splitting water to produce hydrogen [5] magnetic materials [2], [6] anode materials for advanced lithium ion batteries [7]-[8] and high-performance supercapacitors [9]-[10].

Cobalt sulphide thin films have been prepared using several deposition methods as reported by many researchers. Thin films of cobalt sulphide had been deposited by different researchers using various methods such as Chemical Bath Deposition (CBD) technique [1], modified chemical bath deposition route [11], spray pyrolysis method on a glass substrate at constant substrate temperature of 300 °C [12], electrodeposition method onto fluorine doped tin oxide (FTO) [13], sonochemically deposition from $\text{Co}(\text{CH}_3\text{COO})_2 \cdot 2\text{H}_2\text{O}$ and different sulfur precursors using a direct immersion ultrasonic probe [14] and SILAR method onto amorphous glass [15].

In this study, cobalt sulphide (CoS) thin films were deposited on a non-conducting microscopic glass substrates using successive ionic layer adsorption and reaction (SILAR) technique at room temperature. Different cobalt sulphide thin films were deposited under different number of SILAR cycles of 10, 20, 30, 40 and 50 to determine the effect of number of SILAR cycles on the properties of CoS thin films.

This research is motivated by the fact that no literature exists on the effect of SILAR cycles on the properties of CoS thin films. The film growth was based on the reaction between cobalt chloride hexahydrate ($\text{CoCl}_2 \cdot 6\text{H}_2\text{O}$) and sodium sulphide nanohydrate ($\text{Na}_2\text{S} \cdot 9\text{H}_2\text{O}$). The deposited CoS thin films were subjected to optical and structural characterizations with the use of StellarNet UV-VIS-NIR spectrophotometer (Blue-Wave Miniature; Model: UVNb) and X-ray Diffractometer (Bruker D8 Advance X-ray Diffractometer) respectively.

2 Materials and methods

SILAR was employed to fabricate cobalt sulphide thin films. SILAR is an easy, speedy, and cost-effective bottom-up procedure for making nanostructured thin films of binary ternary and composite systems. The SILAR method is mainly based on the adsorption and reaction of the ions from the solutions and rinsing between every immersion with distilled water to avoid homogeneous precipitation in the solution.

In this study, thin films of cobalt sulphide were deposited by the reaction between cobalt chloride hexahydrate ($\text{CoCl}_2 \cdot 6\text{H}_2\text{O}$) and sodium sulphide nanohydrate ($\text{Na}_2\text{S} \cdot 9\text{H}_2\text{O}$), which served as precursors for cobalt ion (Co^{2+}) and sulphide ion (S^{2-}). Triethanolamine (TEA) served as complexing agent at room temperature to slow quick precipitation of cobalt ion when reacted with $\text{Na}_2\text{S} \cdot 9\text{H}_2\text{O}$. 0.20 M solution of the cobalt

ion precursor was prepared by dissolving 4.79 g of $\text{CoCl}_2 \cdot 6\text{H}_2\text{O}$ in 100 mL of distilled water. Similarly, 0.50 M of sulphur ion precursor was prepared by dissolving 12.01 g of $\text{Na}_2\text{S} \cdot 9\text{H}_2\text{O}$ in distilled water. In the cationic precursor, 10 mL of TEA was added to 70 mL of 0.20 M of $\text{CoCl}_2 \cdot 6\text{H}_2\text{O}$. This solution was used as a cationic precursor and the source of Co^{2+} ions and was kept at room temperature, while 80 mL solution of 0.50 M of Na_2S was used as anionic precursor.

Here, five samples were prepared using SILAR cycles of 10, 20, 30, 40 and 50 respectively. At the end of each SILAR cycle, the sample was dried in electric oven at a temperature of 60 °C. A total SILAR cycle time of 160 seconds was maintained for the deposition of the thin films. Figure 2 shows schematic representation of SILAR method adopted to deposit CoS thin films in this present study. One SILAR growth cycle involved four steps enumerated below:

- i. Immersion of the cleaned substrate in first reaction beaker containing cationic precursor solution of 0.2 M [$\text{CoCl}_2 \cdot 6\text{H}_2\text{O}$] for 60s. This process leads to absorption of Co^{2+} ions on the surface of the substrate.
- ii. This substrate was rinsed by high purity distilled water for 20 s to remove excess Co^{2+} ions that are loosely adherent to the glass substrate (achieved in the previous step).
- iii. The substrate was then immersed in the anionic precursor solution of 0.5 M Na_2S for the 60 s. The sulphide (S^{2-}) ions reacted with the absorbed Co^{2+} ions on the active center of the substrate to form CoS films.
- iv. Again, the substrate was rinsed in distilled water for 20 s to remove loosely bound ions present on the substrate and unreacted Co^{2+} and S^{2-} ions.

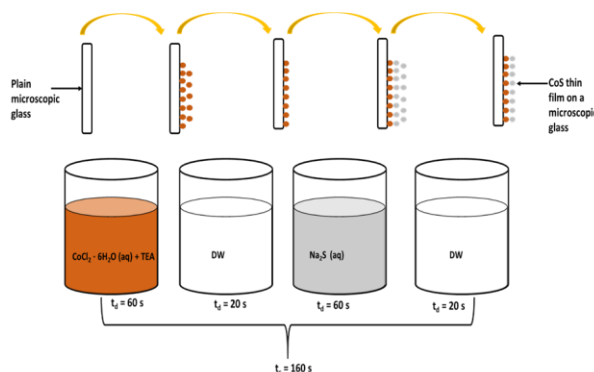
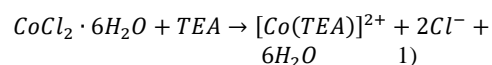
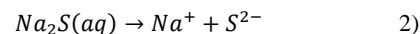


Figure 2: Schematic representation of SILAR method adopted to deposit CoS thin films, t_d = dip time and t_c = cycle time

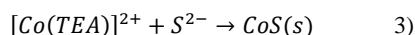
The chemical equation for the formation cobalt sulphide thin film is given as:



Equation (1) shows the complex ion formation when TEA as a complexing agent is added to solution of $\text{CoCl}_2 \cdot 6\text{H}_2\text{O}$.



The $[Co(TEA)]^{2+}$ ion reaction with sulphur ion in Equation (2) to form cobalt sulphide thin films on the surface of the microscopic glass.



After the deposition of the films, optical properties of the deposited cobalt sulphide thin films were studied within the wavelength range of 300 to 1000 nm. The absorbance of the films was obtained using the StellarNet UV–VIS–NIR spectrometer (Blue–Wave Miniature; Model: UVNb). Other optical properties of the deposited thin films were determined using Equations (4)–(8). The deposited CoS thin films were also subjected to structural analysis with the use of X–ray Diffractometer (Bruker D8 Advance X–ray Diffractometer). Thickness values of the deposited film were determined using gravimetric method.

Transmittance (T) values of the deposited thin films were determined using the expression in Equation (4) as given by [16]

$$T = 10^{-A} \quad (4)$$

The expression in Equation (5) as given by [17]–[19] was utilized to determine the reflectance values of the deposited thin films.

$$A + T + R = 1 \quad (5)$$

By employing Equation (6) as given by [20]–[23], the refractive index values of the deposited films were determined.

$$\eta = \frac{1+R}{1-R} + \sqrt{\frac{4R}{(1-R)^2} - k^2} \quad (6)$$

Where R represents the reflectance of the films.

The values of the extinction coefficient (k) for the deposited thin films were determined using Equation (7), as provided by [24], [25]

$$k = \frac{\alpha\lambda}{4\pi} \quad (7)$$

Using Equation (8) as described in [26], [27], the energy bandgap values of SILAR deposited CoS thin films were determined.

$$ahv = A(hv - E_g)^n \quad (8)$$

3 Results and Discussions

3.1 Optical analysis

Figure 3(a) shows the graph of absorbance plotted against wavelength. The graph illustrates the relationship between absorbance and SILAR cycles for deposited films. It indicates that the highest absorbance occurs at 300 nm for films deposited with 50 SILAR cycles, while the lowest absorbance

is observed at 1000 nm for films deposited with 10 SILAR cycles. Increasing the number of SILAR cycles enhances absorbance, allowing the films to effectively absorb UV radiation and potentially be utilized as UV filters [28], [29]. Based on these findings, it can be inferred that increasing the SILAR cycles above 50 could yield highly absorbing CoS thin films.

Figure 3(b) shows the graph of transmittance plotted against wavelength. Transmittance of the films increases sharply as wavelength increased, reaching a peak value between 63.9% at 1000 nm for film deposited at 10 SILAR cycles and minimal transmittance of 19.8% at 300 nm for film deposited at 50 SILAR cycles. Transmittance of the deposited films decreased as the number of SILAR cycles increased. The films show moderate transmittance in VIS region. The observed wide transmission in the entire wavelength region (300 to 1000 nm) enables it to be a potential candidate for optoelectronic applications.

Figure 3(c) shows the graph of reflectance against wavelength. The results indicate that the deposited films exhibit low reflectance overall. Reflectance values range from 0.10, at 300 nm reaching a peak value of 0.2 at 1000 nm for films deposited with 50 SILAR cycles. In the UV and VIS regions, reflectance decreases with an increase in SILAR cycles for all the deposited films.

In the NIR region, films deposited with 10, 20, and 30 SILAR cycles demonstrate a decrease in reflectance as wavelength increases, while films deposited with 40 and 50 cycles show an increase in reflectance values. The low reflectance characteristics of the films suggest their potential use in anti-reflective coatings to remove unwanted electromagnetic radiation. Higher reflectance in the long wavelength region for thicker CoS film and the reverse trend in the lower wavelength region can be attributed to the interference effects that occur within the thin films.

Figure 3(d) shows the graph of refractive index against wavelength. The refractive index, which is a dimensionless number that measures how light propagates through a medium depends on the wavelength of electromagnetic radiation. Generally, the result shows that electromagnetic radiation can propagate through the deposited films at different degrees, i.e. depending on the wavelength.

Within the UV and VIS region, refractive index decreased as number of SILAR cycles increased for all the films deposited. In NIR region, films deposited at 10, 20 and 30 SILAR cycles show a decrease in refractive index as wavelength increased, while films deposited at 40 and 50 cycles show an increase in refractive index values as wavelength increased. The refractive index value ranges from 1.92 at 300 nm to its peak value of 2.64 at 1000 nm for film deposited at 50 SILAR cycles.

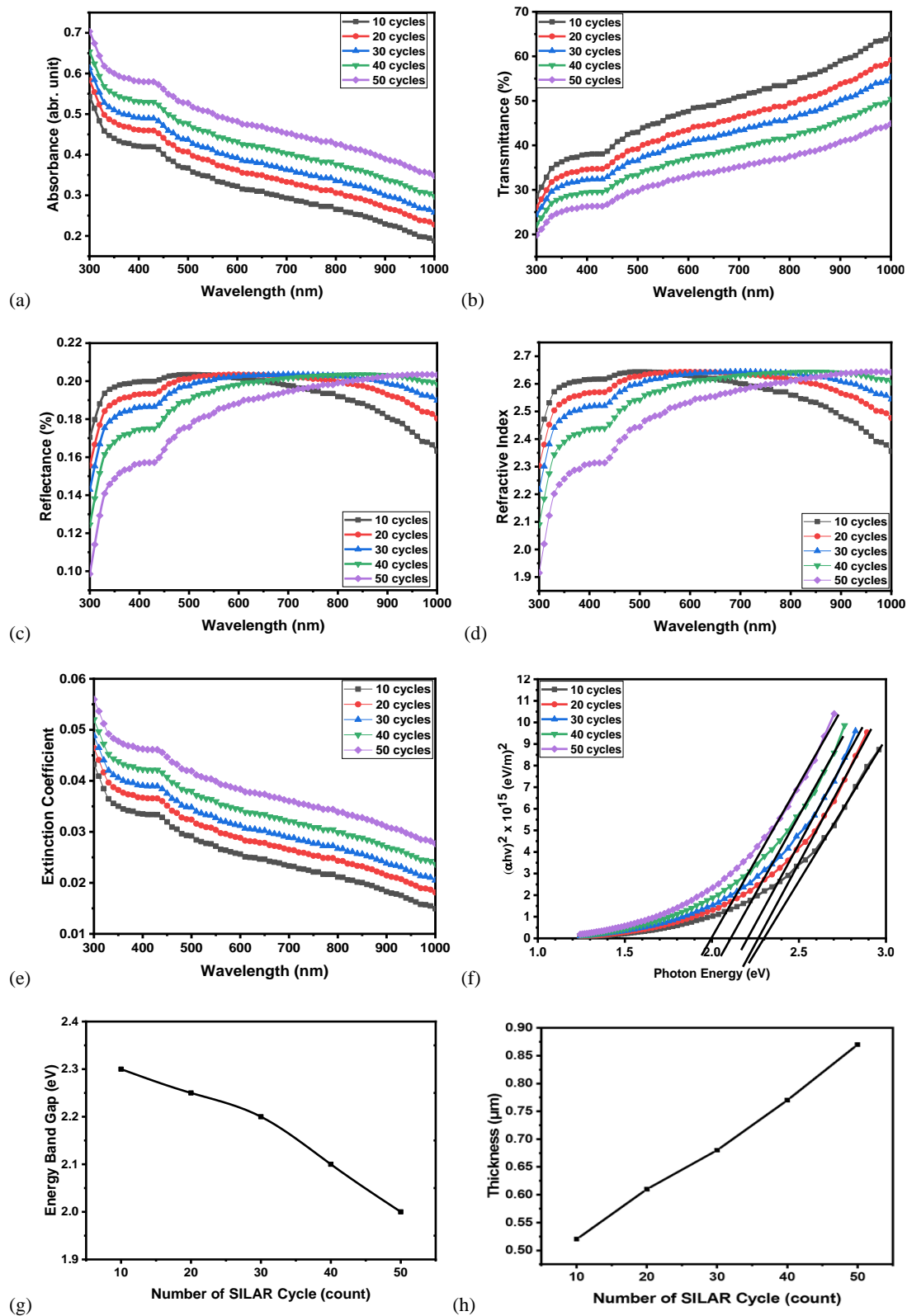


Figure 3: Graph of (a) absorbance (b) transmittance (c) reflectance (d) refractive index (e) extinction coefficient against wavelength (nm) (f) $(ahv)^2$ vs photon energy (g) energy bandgap and (h) thickness (μm) against SILAR cycles for CoS thin films

Figure 3(e) shows the graph of extinction coefficient plotted against wavelength. The extinction coefficient, which is a measure of the degree of absorption of light by the films, depends on the wavelength of the radiation. The result shows that extinction coefficient decreased as wavelength increased, which is a confirmation of the absorption pattern observed for the deposited film. The Extinction coefficient of the films increased as SILAR cycles increased. Extinction coefficient values of 0.056 was obtained at 300 nm for film deposited at 50 SILAR cycles and value of 0.015 was obtained for 10 cycles at 1000 nm.

The optical bandgap energy E_g , of the films were estimated from the plot of square of the product of absorption coefficient and photon energy $(ahv)^2$ versus photon energy (hv) curves shown in Figure 3(f). The straight nature of the plots indicates the existence of direct transition. The direct bandgap energies of as-grown films were determined by extrapolating the straight portion of the photon energy (hv) axis at $(ahv)^2 = 0$. It was found to be between 2.00 – 2.30 eV.

These results show that CoS is a wide bandgap material which could have applications in high power devices, light emitting diodes, optoelectronics, and high frequency devices. These bandgap results are close to the energy bandgap of 1.96 to 2.11 eV obtained by [12]. Energy bandgap of 2.2 eV was obtained by [30], and [29] obtained a bandgap of 1.72 eV for cobalt sulphide thin films.

Figure 3(g) shows the graph of energy bandgap against number of SILAR cycles. The result shows that as the number of SILAR cycles increased, the absorption of CoS thin films shift towards lower energy, a property that was attributed to the quantum confinement effect. The decrease in the energy band gap with increasing thickness of thin film is a consequence of the diminishing quantum confinement effects and the widening availability of energy states for electrons within the films. Similar decrease in energy band gap as number of SILAR cycles increases has been reported by [31].

Table 1 shows the variation of number of SILAR cycle with thickness and energy bandgap. The thickness of the films was evaluated using gravimetric approach as given by [32], [33]. The results show that the energy bandgap decreased as the thickness of the films increased.

Table 1: Variation of SILAR cycle with thickness and energy bandgap

SILAR cycles	Thickness (μm)	Energy Bandgap (eV)
10	0.52	2.01
20	0.61	1.96
30	0.68	1.90
40	0.77	1.85
50	0.87	1.82

Figure 3(h) shows the graph of average optical thickness against number of SILAR cycles. Film thickness increased with the increase in the number of SILAR cycles. Peak thickness of 0.87 μm was obtained for film deposited at 50

SILAR cycles and least thickness of 0.52 μm was obtained for film deposited at 10 SILAR cycles.

3.2 Structural analysis

The X-ray diffraction spectra of the deposited cobalt sulphide thin films at 10, 30 and 50 SILAR cycles is shown in Figure 4(a). The X-ray diffraction spectra shows peaks corresponding to the reflections of hexagonal phase of CoS with JCPDS file number (01-075-0605) and lattice parameter $a=b=3.370 \text{ \AA}$ and $c=5.140 \text{ \AA}$. The planes have miller indices of (100), (101), (102), (110) and (202) corresponding to the 2θ angles of 30.57° , 35.51° , 46.62° , 53.42° and 72.56° respectively. The preferred orientation is along the [102] plane. The strong and sharp diffraction peaks demonstrate that the films are crystalline in nature. The increase in the intensity of the films as SILAR cycles increased suggests that the crystallinity of the films increase as SILAR cycle increases. Similar hexagonal phase of CoS thin films was obtained by [34], [35].

The Bragg peak breadth is a combination of both instrument and sample dependent effects. To take care of these aberrations, it is needed to assemble a diffraction pattern from the line broadening of a standard material such as silicon (111) to determine the instrumental broadening. The instrument corrected broadening β_D corresponding to the diffraction peaks is given by [36] as

$$\beta_D^2 = [\beta_{\text{measure}}^2 - \beta_{\text{instrument}}^2] \quad (9)$$

$$D = \frac{k\lambda}{\beta_D \cos \theta} \Rightarrow \cos \theta = \frac{k\lambda}{D} \left(\frac{1}{\beta_D} \right) \Rightarrow \beta_D = \frac{k\lambda}{D \cos \theta} \quad (10)$$

While the crystal imperfection and distortion of strain-induced peak broadening are related by

$$\varepsilon = \frac{\beta_s}{\tan \theta} \quad (11)$$

Where D is the crystallite size (grain size), λ is the wavelength of the X-ray radiation, θ is the angle of diffraction.

The extraordinary property of Equation (9) is its dependency on the diffraction angle θ . Depending on different θ positions, the separation of size and strain broadening analysis is done using Williamson–Hall method. Where Equations (9), (10) and Scherrer equations are combined, we have that

$$\begin{aligned} \beta_{hkl} &= \beta_s + \beta_D \\ \beta_{hkl} &= \left(\frac{k\lambda}{D \cos \theta} \right) + 4\varepsilon \tan \theta \\ \beta_{hkl} \cos \theta &= \left(\frac{k\lambda}{D} \right) + 4\varepsilon \sin \theta \\ \beta \cos \theta &= \frac{0.9\lambda}{D} + 4\varepsilon \sin \theta \end{aligned} \quad (12)$$

Where β is the full width at half maximum, ε is the microstrain. A plot of $\beta \cos \theta$ against $4 \sin \theta$, which is the Hall–Williamson plot, gives the slope of the graph to be equal to the microstrain ε and the intercept on the $\beta \cos \theta$ axis equals to $\frac{0.9\lambda}{D}$.

Therefore, the crystallite size is given as

$$D = \frac{0.9\lambda}{\text{intercept on } \beta \cos \theta \text{ axis}} \quad (13)$$

From the plots in Figure 4(b-d), the crystallite sizes were found to be 32.25, 36.49 and 40.78 nm. Dislocation density of the films was found to be 9.61×10^{14} , 7.51×10^{14} and 6.01×10^{14} lines/m² while microstrain values obtained were 2.00×10^{-4} , 5.00×10^{-4} and 7.00×10^{-4} respectively.

The crystallite size and microstrain of the films were found to increase as SILAR cycle increases while dislocation densities were found to decrease as number of SILAR cycles increases. Low values of microstrain suggest that the films deposited have little or no defects. The positive slope in Figure 12 indicates tensile strain within the crystal structure of the films. The results of the X-ray diffraction of the deposited samples correspond with those obtained by [11], [30], and [37].

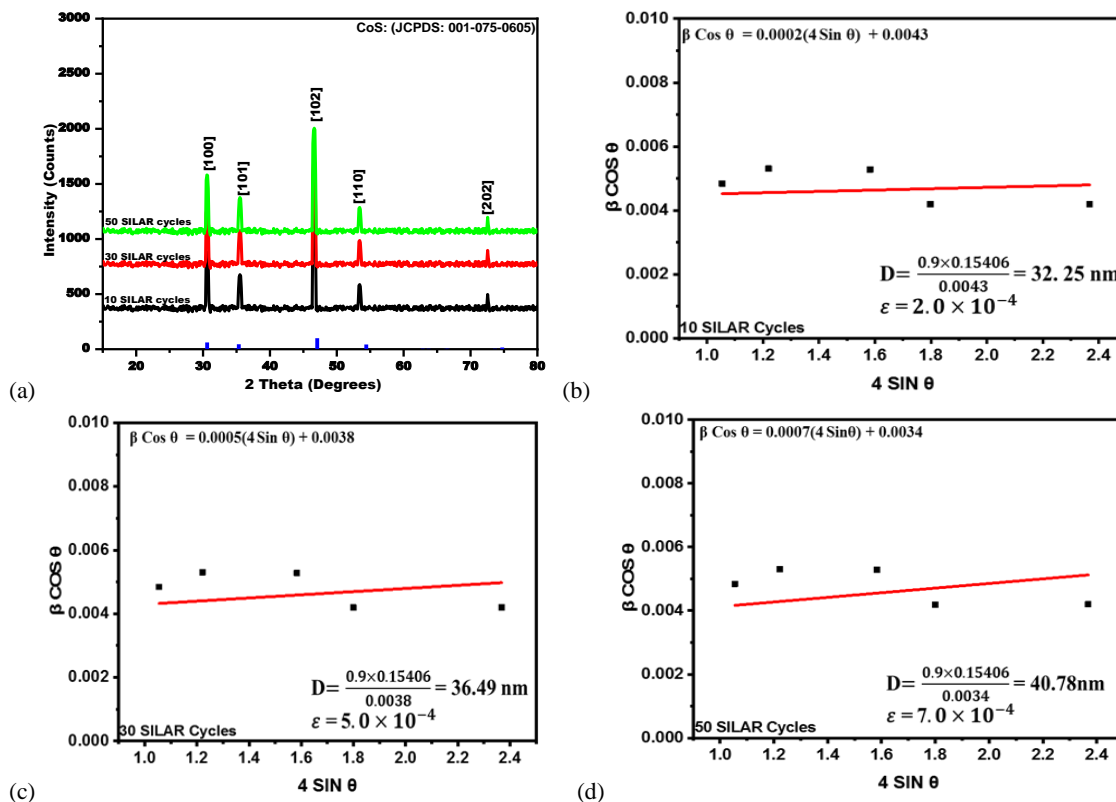


Figure 4: (a) X-ray diffractograms (b-d) Williamson–Hall plots of the deposited cobalt sulphide for 10, 30 and 50 SILAR cycles

4 Conclusions

We have successfully deposited thin film of cobalt sulphide (CoS) thin films on a non-conducting microscopic glass substrates using SILAR technique. Deposition of CoS thin films was done at room temperature (300 K) using cobalt chloride hexahydrate ($\text{CoCl}_2 \cdot 6\text{H}_2\text{O}$), sodium sulphide ($\text{Na}_2\text{S} \cdot 9\text{H}_2\text{O}$) as precursor for cobalt and sulphur respectively.

The deposited films of CoS thin films were subjected to optical characterizations which showed that cobalt sulphide films are moderately absorbing films. The absorbance results demonstrated that the cobalt sulphide films exhibit moderate absorption properties, with absorbance values ranging from 0.70-0.19 abr. unit. The transmittance measurements indicated that these films are fairly transparent in the visible light and near-infrared regions, with transmittance values ranging from 19.8% to 63.9%. Furthermore, the transmittance decreased as the number of SILAR cycles increased. The reflectance of the

synthesized films was generally low, ranging between 0.10 and 0.20, indicating their potential for anti-reflective applications. The refractive index within the UV and VIS regions decreased as the number of SILAR cycles increased for all the deposited films. The refractive index value ranged from 1.92 at 300 nm to its peak value of 2.64 at 1000 nm. The bandgap energy of the deposited films ranged from 2.00 – 2.30 eV, providing valuable information for optoelectronic applications. Additionally, the optical thickness of the films increased with an increase in the number of SILAR cycles, ranging from 0.52 μm to 0.87 μm .

On the other hand, structural analysis revealed that the XRD pattern of the deposited CoS thin films exhibited peaks corresponding to the reflections of the hexagonal phase of CoS with lattice parameters of $a=b=3.377 \text{ \AA}$ and $c=5.150 \text{ \AA}$. The preferred orientation was observed along the [102] plane. Using the Williamson-Hall plot method, the crystallite sizes, microstrain, and dislocation density of the films were

determined, ranging from 32.25 to 40.78 nm, 2.0×10^{-4} – 7.0×10^{-4} and 9.61×10^{14} – 6.01×10^{14} lines/m².

Thus, this study provides comprehensive optical and structural characterizations of CoS thin films deposited via SILAR, highlighting their potential for various applications in optoelectronics, anti-reflective coatings, and beyond. Further research and optimization can be pursued to explore their potential in diverse technological fields.

Declaration of Competing Interest

The authors declare no personal or financial conflicts that may influence the research presented in this paper.

References

- [1] Govindasamy G., PriyaMurugasenb, Suresh Sagadevan, (2017). Optical and Electrical Properties of Chemical Bath Deposited Cobalt Sulphide Thin Films. *Materials Research*. 20(1), 62 – 67.
- [2] Bao, S.-J., Li, Y., Li, C.M., Bao, Q., Lu, Q. & Guo J., (2008). Shape evolution and magnetic properties of cobalt sulphide. *Crystal Growth Design*, 8, 3745 – 3749.
- [3] Hoodless, R.C., Moyes, R. B. & Wells, P. B., (2006). D-tracer study of butadiene hydrogenation and tertahydrothiophen hydrodesulphurization catalysed by Co_9S_8 . *Catalysis Today*, 114, 377 – 382.
- [4] Patil, S. A., Shinde, D. V., Lim, I., Cho, K., Bhande, S. S., Mane, R. S., Shresta, N. K., Lee, J. K., Yoon, T. H. & Han, S. H., (2015). An Ion Exchange Mediated Shape- perserving Strategy for Constructing 1-D Arrays of Porous $CoS_{1.0365}$ Nanorods for Electrocatalytic Reduction of Triiodide. *Journal of Material Chemistry*, A3, 7900 – 7909
- [5] Feng, L. L., Li, G. D., Liu, Y. P., Wu, Y. Y., Chen, H., Wang, Y., Zou, Y. C., Wang, D. J. & Zou, X. X., (2015). Carbon-armed Co_9S_8 nanoparticles as all-pH efficient and durable H_2 -evolving electrocatalysts. *ACS Applied Material Interfaces*, 7, 980 – 988. DOI: <https://doi.org/10.1021/am507811a>
- [6] Rumale, N, Arbuj, S., Umarji, G., Shinde, M., Mulik, U., Joy, P. & Amalnerkar, D., (2015). Tuning Magnetic Behavior of Nanoscale Cobalt Sulfide and its Nano-composite with an Engineering Thermoplastic. *Journal of Electronic Material*, 44, 2308 – 2311. DOI: <https://doi.org/10.1007/s11664-015-3753-1>
- [7] Wang, Q., Zou, R., Xia, W., Ma, J., Qiu, B., Mahmood, A., Zhao, R., Yang, Y., Xia, D. & Xu, Q., (2015). Facile synthesis of ultra – small CoS_2 nanoparticles within thin N- doped porous carbon shell for high performance lithium-ion batteries. *Small*, 11(21), 2511 – 2517. DOI: <https://doi.org/10.1002/smll.201403579>
- [8] Li, Z. P., Li, W. Y., Xue, H. T., Kang, W. P., Yang, X., Sun, M. L., Tang, Y. B. & Lee, C. S., (2014). Facile fabrication and electrochemical properties of high quality reduced graphene-oxide / cobalt sulphide composite as anode material for lithium-ion batteries. *Royal Society of Chemistry Advances*, 4, 37180 – 37186. DOI: <https://doi.org/10.1039/C4RA06067A>
- [9] Chen, Q., Li, H., Cai, C., Yang, S., Huang, K., Weiab, X. & Zhong, J., (2013), Insitu shape and phase transformation synthesis of Co_3S_4 nanosheet arrays for high performance electrochemical supercapacitors, *Royal Society of Chemistry Advances*, 3(45), 22922 – 22926. DOI: <https://doi.org/10.1039/C3RA44237C>
- [10] Wan, H., Ji, X., Jiang, J., Yu J., Miao, L., Zhang, L., Bie, S., Chen, H. & Ruan, Y., (2013). Hydrothermal synthesis of cobalt sulphide nanotubes; the size control and its application in supercapacitors. *Journal of Power Sources*, 243, 396 – 402. DOI: <https://doi.org/10.1016/j.jpowsour.2013.06.027>
- [11] Sonawane, M. S., Baviskar, P. K. & Patil, R. S. (2016), Synthesis of Cobalt Sulphide Thin Film Electrode by Modified Chemical Bath Deposition Route and its Supercapacitors Performance. *International Journal of Advanced Research*, 4(12), 679 – 686. DOI: <http://dx.doi.org/10.21474/IJAR01/2446>
- [12] Sattar, M. A., Mozibur, R. M., Khan, M. K. R. & Choudhury, M. G. M. (2014). Optical Characterization of Spray Deposited CoS Thin Films. *International Journal of Recent Technology and Engineering*, 2(6), 10 – 13.
- [13] Karim, N. A., Ludin, N. A., Mat-Teridi, M. A., Sepeai, S., Ibrahim M. A., Kouhnavard M., Sopian K. & Arakawa H., (2018), Effects of Deposition Time on Cobalt Sulfide Thin Film Electrode Formation. *Malaysian Journal of Analytical Sciences*, 22(1), 80 – 86. DOI: <https://doi.org/10.17576/mjas-2018-2201-10>
- [14] Kristl, M., Dojer, B., Gyergyek, S. & Kristl, J., (2017). Synthesis of nickel and cobalt sulfide nanoparticles using a low cost sonochemical method. *Heliyon*, 3(3), Article No. – e00273. DOI: <https://doi.org/10.1016/j.heliyon.2017.e00273>
- [15] Sartale, S. D. & Lokhande, C. D., (2000). Deposition of Cobalt Sulphide Thin Films by Successive Ionic Layer Adsorption and Reaction (SILAR) method and their Characterization. *Indian Journal of Pure and Applied Physics*, 38, 48 – 52.
- [16] Nwori, A. N., Ezenwaka, L. N., Ottih, I. E., Okereke, N. A. & Okoli, N. L. (2022). Study of the Optical, Structural and Morphological Properties of Electrodeposited Copper Manganese Sulfide (CuMnS) Thin Films for Possible Device Applications. *Trends in Sciences*, 19(17), 5747. DOI: <https://doi.org/10.48048/tis.2022.5747>
- [17] Ijeh, R. O., Nwanya, A. C., Nkele, A. C., Madiba, I. G., Khumalo, Z., Bashir, A. K. H., Osuji, R. U., Maaza, M. & Ezema, F. I. (2019). Magnetic and optical properties of electrodeposited nanospherical copper doped nickel oxide thin films. *Physica E: Low-dimensional Systems*

- and Nanostructures, 113, 233-239. DOI: <https://doi.org/10.1016/j.physe.2019.05.013>
- [18] Shinen, M. H., Alsaati, S. A. A. & Rasooqi, F. Z. (2018). Preparation of high transmittance TiO₂ thin films by Sol gel Techniques as antireflection coating. *Journal of Physics, Conference Series*, 1032, 1-11. DOI: <http://dx.doi.org/10.1088/1742-6596/1032/1/012018>
- [19] Al – Dahaan, S. A. J, Al-khayatt, A. H. O & Salman, M. K. (2014). The optical Properties of Fe₂O₃ Thin Film Prepared by Chemical spray pyrolysis Deposition (CSP). *Journal of Kufa-Physics*, 6(2), 16-23.
- [20] Guneri, E. & Kariper, A. (2013). Characterization of high quality Chalcogenide thin films fabricated by Chemical Bath Deposition. *Electronic Materials Letters*, 9(1), 13-17. DOI: <https://doi.org/10.1007/s13391-012-2099-6>
- [21] Augustine, C., Nnabuchi, M. N., Chikwenze, R. A., Anyaegbunam, F. N. C., Kalu, P. N., Robert, B. J., Nwosu, C. N., Dike, C. O. & Taddy, E. N. (2019). Comparative investigation of some selected properties of Mn₃O₄/PbS and CuO/PbS composites thin films. *Material Research Express*, 6, 1-10. DOI: <https://doi.org/10.1088/2053-1591/ab1058>
- [22] Kariper, I. A. (2017). Synthesis and characterization of CrSe thin film produced via chemical bath deposition. *Optical Review*, 24(2), 139-146. DOI: <https://doi.org/10.1007/s10043-017-0307-1>
- [23] Kariper, I. A. (2018). A new Route to Synthesis MnSe Thin films by Chemical Bath Method. *Material Research*, 21(2), 1 – 6. DOI: <http://dx.doi.org/10.1590/1980-5373-MR-2017-0215>
- [24] Howlader, C., Hasan, M., Zakhidov, A., & Chen, M. Y. (2020). Determining the refractive index and the dielectric constant of PPDT2FBT thin film using spectroscopic ellipsometry. *Optical Materials*, 110, 110445. DOI: <https://doi.org/10.1016/j.optmat.2020.110445>
- [25] Omar, E., Ahmed, A., Diab, A., & Mohamed, H. (2023). Study of the Effect of Thickness on the Optical Properties of MnBi_{0.95}Sb_{0.05} Thin Film. *Sohag Journal of Sciences*, 8(2), 157-161. DOI: <https://doi.org/10.21608/sjsci.2023.179767.1046>
- [26] Tauc, J., Grigorovici, R. & Vancu, A. (1966). Optical Properties and Electronic Structure of Amorphous Germanium. *Physics Status Solid*. 15(2), 627–637. DOI: <https://doi.org/10.1002/pssb.19660150224>
- [27] Tezel, F. M., Ozdemir, O. & Kariper, I. A. (2017). The Effects of pH on Structural and Optical Characterization of Iron oxide Thin Films. *Surface Review and Letters*, 24(4), 1-10. DOI: <https://doi.org/10.1142/S0218625X17500512>
- [28] Nnabuchi, M. N. & Ekuma, C. E. (2010). Synthesis and Characterization of Chemical Bath Deposited CdCoS thin film. *Chalcogenide Letters*, 7, 31 – 38.
- [29] Okoli, D. N. & Okoli, C. N. (2012). Optimal Growth and Characterization of Cobalt Sulphide Thin Films Fabricated Using the Chemical Bath Deposition Technique, *Journal of Natural Sciences Research*, 2(3), 5 – 9.
- [30] Sonawane, M. S. & Patil, R. S. (2014), Characterization of Chemically Deposited Nanocrystalline Cobalt Sulphide Thin Films. *International Journal of Advanced Scientific and Technical Research*, 3(4), 57 – 64.
- [31] Egwunyenga, N. J., Onuabuchi, V. C., Okoli, N. L., & Nwankwo, I. E. (2021). Effect of SILAR cycles on the thickness, structural, optical properties of cobalt selenide thin film. *International Research Journal of Multidisciplinary Technovation*, 10, 1-9. DOI: <https://doi.org/10.34256/irjmt2141>
- [32] Ezenwaka, L. N., Okoli, N. L., Okereke, N. A., Ezenwa, I. A. & Nwori, N. A. (2021). Properties of Electrosynthesized Cobalt Doped Zinc Selenide Thin Films Deposited at Varying Time. *Nanoarchitectonics*, 3(1), 1 – 9. DOI: <https://doi.org/10.37256/nat.3120221040>
- [33] Okoli, N. L., Nkamuo, C. J., Elekalachi, C. I., & Obimma, I. O. (2022). Influence of Annealing Temperature on the Optical, Structural, Morphological and Compositional Properties of SILAR Deposited Copper Manganese Oxide Thin Films. *Journal of Nano and Materials Science Research*, 1, 68–75. Retrieved from <http://journals.nanotechunn.com/index.php/jnmsr/article/view/8>
- [34] Kamble, S. S., Sikora, A., Pawar, S. T., Kambale, R. C., Maldar, N. N., & Deshmukh, L. P. (2015). Morphology reliance of cobalt sulfide thin films: A chemo-thermo-mechanical perception. *Journal of Alloys and Compounds*, 631, 303–314. DOI: <https://doi.org/10.1016/j.jallcom.2015.01.097>
- [35] Kamble, S. S., Dubal, D. P., Tarwal, N. L., Sikora, A., Jang, J. H., & Deshmukh, L. P. (2016). Studies on the Zn_xCo_{1-x}S thin films: A facile synthesis process and characteristic properties. *Journal of Alloys and Compounds*, 656, 590–597. DOI: <https://doi.org/10.1016/j.jallcom.2015.10.011>
- [36] Prablu, Y. T., Rao, K. V., Kumar, V. S. S. & Kumari, B. S., (2014). X – ray Analysis by Williamson – Hall and Size – Strain Plot Methods of ZnO Nanoparticles with Fuel Variation. *World Journal of Nano Science and Engineering*, 4, 21 – 28. DOI: <https://doi.org/10.4236/wjnse.2014.41004>
- [37] Kale, S. B., Lokhande, A. C., Pujari, R. B. & Lokhande, C. D. (2018). Cobalt Sulfide Thin Films for Electrocatalytic Oxygen Evolution Reaction and Supercapacitor Applications. *Journal of Colloid and Interface Science*, 532, 491–499. DOI: <https://doi.org/10.1016/j.jcis.2018.08.012>